Spontaneous Droplet Jump with Electro-bouncing

Erin S. Schmidt[1]†, and M. W. Weislogel[1]

[1]Department of Mechanical Engineering, Portland State University, Portland, OR 97211, USA

(Received xx; revised xx; accepted xx)

We investigate the dynamics of water droplet jumps from superhydrophobic surfaces in the presence of an electric field during a step reduction in gravity level. In the brief free-fall environment of a drop tower, when a strong non-homogeneous electric field (with a measured strength between 0.39 and 2.36 kV/cm) is imposed, body forces acting on the jumped droplets are primarily supplied by polarization stress and Coulombic attraction instead of gravity. The droplet charge, measured to be on the order of $2.3 \cdot (10^{-11})$ C, originates by electro-osmosis of charged species at the (PTFE coated) hydrophobic surface interface. This electric body force leads to a droplet bouncing behavior similar to well-known phenomena in 1-g, though occurring for larger drops $\sim$0.1 mL for a given range of impact Weber numbers, $\mathbf{We} < 20$. In 1-g, for $\mathbf{We} > 0.4$, impact recoil behavior on a super-hydrophobic surface is normally dominated by damping from contact line hysteresis and by air-layer interactions. However, in the strong electric field, the droplet bounce dynamics additionally include electrohydrodynamic effects on wettability and Cassie-Wenzel transition. This is qualitatively discussed in terms of coefficients of restitution and trends in contact time.

Electrostatic forces present opportunities for the study and control of unique μ-gravity droplet dynamics. Unfortunately, in many cases such forces manifest as a complicating nuisance variable. In the present work, the sources and magnitudes of these effects are surveyed, and options for avoiding or mitigating them are presented. Additionally a scale quantity of concern is presented for rapid estimation of limiting behaviors for droplet kinematics dominated by electrostatic forces; pertinent terms in the scale quantity include droplet charge and electric field strength. The strength of electric fields originating from static charge on acrylic surfaces used in drop tower experiments was measured using an electrostatic field meter. The mean electric field strength sampled at 25 mm away from a population of surfaces is 150 V, however the field strength ranges from 10 V (at the limit of sensor accuracy) to over 3 kV. The electrostatic force, and thus the total charge in the droplet was revealed by observation of the accelerations of droplets in a homogeneous electric field of known strength. Typical droplet net charge, supposedly developed through electro-osmosis of charged ionic species from the PTFE treated hydrophobic surfaces, was measured to be 2.3e-11 C with a standard deviation of 1.8e-11 C.

1. Introduction

When a nonwetting, gravity dominated sessile drop or puddle initially at rest in the Cassie-Baxter state on a surface undergoes a large step reduction in Bond number, $\mathbf{Bo} = \rho g V_d^{2/3}/\sigma$, where ρ is the liquid density, g is the acceleration of gravity, V_d is the droplet volume, and σ is the liquid surface tension, it will spontaneously jump away from the surface. This was first observed experimentally by Kirko *et al.* in 1970 [ref] and later

† Email address for correspondence: esch2@pdx.edu

FIGURE 1. Droplet jump velocities, effect of hysteresis for small droplet size

by Wollman *et al.* in 2006 in a set of experiments conducted using a μ-gravity drop tower[ref]. The kinetic energy of the jump is supplied by the defect in free surface energy as the new minimum energy surface equilibrium has approximately constant curvature [ref]. If the viscous energy losses by shear, and internal flows during roll up are neglected, as well as energy lost due to the hysteresis of the dynamic contact line, then the energy relation is given by

$$KE = SE_2 - SE_1 = [(\sigma A)_{gl} + (\sigma A)_{sg}]_2 - [(\sigma A)_{ls} + (\sigma A)_{gl} + (\sigma A)_{sg}]_1.$$

From this is derived a simple model for the droplet initial jump velocity, given by

$$U_0 = \left(\frac{\sigma g}{\rho}\right)^{1/4} \left[1 - \cos\theta + 2\left(\frac{\pi H^3}{V_d}\right)^{1/2} - 6^{2/3}\left(\frac{\pi H^3}{V_d}\right)^{1/3}\right]^{1/2}.$$

The droplet 'rolls up' as it jumps away from the surface due to radial motion of capillary wave away from the contact line. The characteristic time scale of the rolling up scales as $t_j \sim R_p/U\ (\rho H R_p^2/\sigma)^{1/2}$ [ref], which resembles the contact time, $\tau \approx 2.6(\rho R_d^3/\sigma)^{1/2}$ reported by Richard *et al.* in 2002 for the related problem of droplets impacting hydrophobic surfaces in 1-g. For droplets with radial symmetry and sufficiently high initial **Bo** these waves coalesce as a shock leading to geyersing and creation of satellite drops by the Rayleigh-Plateau breakup of the geyser. In the case of smaller jumping droplets, the capillary waves do not lead to geyersing, and are viscously damped to varying degrees during the brief freefall period of the drop tower.

The spontaneous droplet jump phenomenon provides a useful window though which to study the dynamics of large-lengthscale capillary dominated droplets. The governing physics of such massive droplets (far beyond the 1-g sub-millimetric capillary lengthscale) utterly defy terrestrial expectations about the ways in which liquid droplets 'should' behave, and also are of critical importance in a space exploration setting where the design of practical μ-gravity multiphase fluidic systems will no doubt be needed as humankind gradually extends her domain into the rest of the solar system.

The μ-gravity conditions useful for the study of droplet kinematics can be accessed, albeit briefly, in a drop tower facility such as Portland State Uni- versitys Dryden

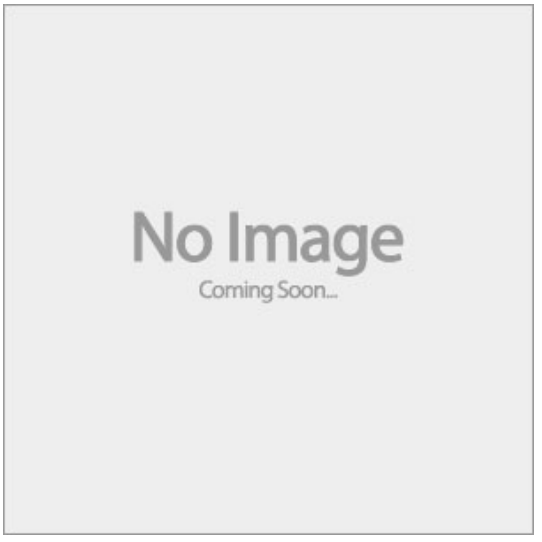

FIGURE 2. μ-gravity drop tower

Drop Tower. In drop tower experiments, as well as in experiments conducted in a true space environment, anomalous accel- erations are a potential subject of concern to experimentalists studying droplet kinematics. This is especially true in the study of droplets of small inertia which may be subject to environmental factors that are difficult to control empirically. While there is nothing overtly mysterious about the underlying forces causing such droplets to accelerate, the forces must nevertheless be mitigated or accounted for. Spontaneous droplet jump, droplet dynamics are usually dominated by inertia, however spurrious forces were occasionally observed.

Electrohydrodynamic forces, like thermocapillary forces, are useful in μ-gravity where, due to the absence of bouyancy the locations of droplet and bubbles, and other stray interfaces need to be controlled by various means. This is the famous phase seperation problem of μ-gravity.

Under μ-gravity conditions unique force balances act on droplets revealing dynamics difficult to study at macro-scales in a terrestrial environment. The study of droplet dynamics in μ-gravity is thus of interest to many areas of basic research. For acceleration of droplets in μ-gravity forces other than gravity are required. Aerodynamic force contributions include drag and lift, virtual mass effects, Basset forces due to developing boundary layers, and additional exotic forms of drag that are encountered in dynamics of combusting droplets, such as Stefan drag, thermophoresis effects, and droplet-soot interactions **?**. Droplets can also be entrained by large scale eddy and wake structures due to participating gas phase inertia. Surface forces can also be imposed by the presence of strong acoustic fields.

Water is one of the principle model fluids used in μ-gravity droplet dynamics research. Body forces acting on water droplets may be imparted by the presence of an electric field. Water molecules are dipoles and are thus influenced by the presence of non-homogeneous electric fields. Additional forces may develop due to dielectrophoresis, and due to Coulombic forces arising from the presence of static charge on the surface of the droplets themselves. While aboard the International Space Station NASA Flight Engineer Pettit experimented with Coulombic orbiting of droplets charged to high voltage around a knitting needle similarly charged, but with the opposite polarity and using the triboelectric effect **?**.

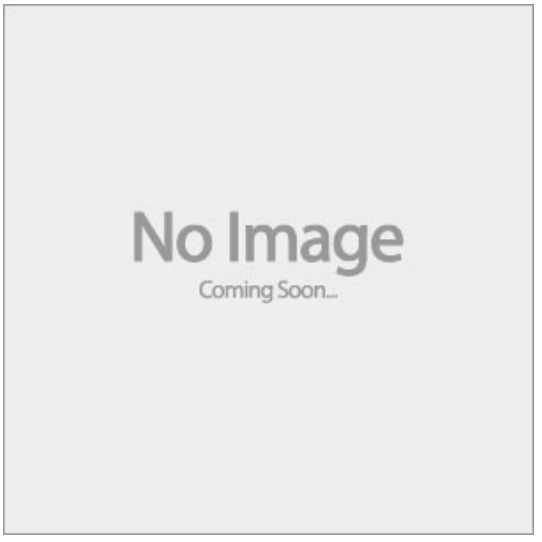

FIGURE 3. Composite photograph showing a bouncing droplet

Droplet dynamics which appear to be strongly influenced by electrostatic forces have also been observed at Portland State University's Dryden Drop Tower (DDT) facility. These experiments follow from earlier research done at the DDT measuring velocities of droplets jumped from hydrophobic surfaces during step-reductions in gravitational acceleration **?**. In this case the presence of strong forces beyond surface tension and droplet inertia are important nuisance variables that must be mitigated or otherwise properly accounted for. Previous experiments in the DDT examining aerodynamic effects on droplets jumped from hydrophobic surfaces noted the presence of anomalous accelerations for a large data set of 0.1 mL droplets. The source of these accelerations was not captured entirely by aerodynamic drag effects, though the presence of an acrylic 'eddy shield' did have a statistically significant effect on the mean droplet accelerations. The effect of static charge appeared, at least qualitatively, to be a significant confounding variable in determining the contribution of aerodynamics to droplet accelerations.

The Dryden Drop Tower, patterned on the 2.2 Second Drop Tower facility at NASA's Glenn Research Center in Cleveland, Ohio, is optimized for exceptionally fast drop turnaround times. The DDT is one of the most productive drop towers in the world for its class, with more than 7000 drops over its XX year history. The DDT's 2.1 seconds of free-fall conditions provide unique opportunities for the observation of phenomena that are usually masked at the macro-scale in 1-g gravity fields. In addition to the DDT itself, an institutionally ingrained rapid prototyping "Fail Fast, Fail Often" iterative design philosophy underpins much of this lab's productivity. In the context of the present study this rapid prototyping approach includes widespread use of lasercut acrylic surfaces, and in-house fabricated PTFE treated super-hydrophobic surfaces. Unfortunately, acrylic surfaces and PTFE spray treatments in particular lend themselves to accumulation of large amounts of static charge which affects droplet kinematics. The object of the current study then is to provide the DDT lab with a means of sanitizing droplet kinematic data from the confounding effects of electrostatic fields, and to identify regimes where there is some assurance that the effect of such fields is small. This can be aided by the empirical determination of scale quantities of concern for the flow.

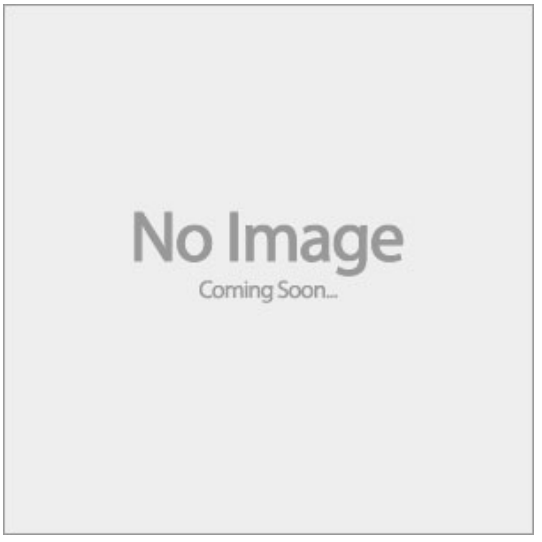

FIGURE 4. Comparison of droplet trajectories, as a function of mass

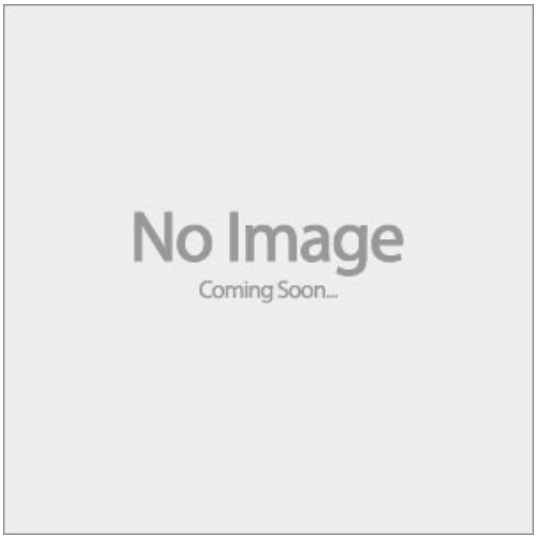

FIGURE 5. 3D plot of interacting droplet pair

1.1. *Force due to an electric field*

Electrohydrodynamic concerns the flow of liquid dielectrics subject to electric fields. These have have been studies with an eye towards space applications in [ref][ref][ref][ref].

The electric body forces acting on the droplets are Laplace's equation

$$\nabla^2 \phi = 0$$

Where the boundary conditions are given values of the potential in the far field, and the surface charge density of the dielectric surface. The electric field is defined as the negative of the gradient of the potential

$$\mathbf{E} = -\nabla \phi$$

[notes on the field for the square geometry]

Momentum conservation confirms that the electric volumetric body force is the same obtained by integrating the momentum flux density over the surface confining the liquid. Thus the total body force for a fluid volume can be estimated by. The total force acting on the droplet can be calculated in the most rigerous fashion from the Maxwell stress tensor, where the total electric force is the obtained by integrating the stress tensor over the surface of the droplet,

$$\mathbf{F}_{DEP} = \oint (\tau_m \cdot \mathbf{n}) d\Gamma.$$

The Maxwell stress tensor τ_m is usually expressed as

The EHD approximation usually makes the fundamental assumption that currents in the medium are so weak that the magnetic field they induce is so weak as to be neglected. We also assume that the system is isothermal, and there is no gradient in the permittivity due to thermal gradient. What that assumption we have

$$\tau_m = \epsilon_0 \epsilon \left(\mathbf{E}_i \mathbf{E}_j - \frac{1}{2} \delta_{ij} E^2 \right)$$

The electric body force is then

$$\mathbf{F}_{elec} = \rho_c \mathbf{E} - \frac{1}{2} E^2 \nabla \epsilon$$

This is regarded as the most rigerous approach for deriving the forces induced by the electric field.

The equations governing the motion of the jumped droplet are the momentum equation and Maxwell's equations. The electrostatic forces described by Maxwell's equations are those arising from free charge in an external electric field (the Coulombic force), and those arising due to polarization effects. In the droplet bounce phenomenon described here we suppose first that dynamic currents are so low that the effect of magnetic fields can be safely neglected. For this approximation to apply the characteristic time scale for electrical phenomenon $\tau = \epsilon/\sigma$, must be small, where we note that τ is the ratio of dielectric permeability to conductivity of the medium. For the conductivity of air ($\sigma = 2.5 \cdot 10^{-16}\ \Omega^{-1} cm^{-1}$), we estimate $\tau \approx 400$s. This assumption also allows us to assume that the net charge present in the sorrounding medium remains approximately constant during the typical time interval of a μ-gravity experiment.

Once the electric potential has been calculated we find the body force density from the Korteweg-Helmholtz formulation of the Maxwell stress integral, given by

$$\mathbf{F} = \rho \mathbf{E} - \frac{1}{2} E^2 \nabla \epsilon + \nabla \left(\frac{1}{2} \mathbf{E} \cdot \mathbf{E} \frac{\partial \epsilon}{\partial \rho} \right)$$

The final term is the electrostriction force density, which can be ignored for incompressible flows. Though this equation nominally adds a level of coupling between to momentum equation as the electric body force source term is a function of the electric field, but the field itself is perturbed as the droplet (and its accompanying net charge) is convected through space. We henceforth assume that the perturbed field due to the droplet charge is a high order correction to the basic field, and is neglected. The first term in xx is due to net charge residing on the droplet, where as the second term is due to polarization of the droplet in a nonuniform electric field, dielectrophoresis.

Dielectrophoresis is the motion of matter in a nonuniform electric field due to polarization of a dielectric. The most polar material migrates toward the region of greatest field intensity. The relative permittivity of the particle compared to the surrounding medium determines the direction of the induced dipole/multipole moment with respect to the

applied field. Depeding on this alignment the particle will experience wither an attractive force or repelling force towards the regions of higher electric field. Unlike electrophoresis caused by the Coulombic force, dielectrophoresis does not require any net charge to be present on the droplet. Any dipole (whether induced or permanant) will have some finite, equal seperation of charge in it. The electric field will cause an alignment of the dipole with it; because the field is nonuniform, on end of the dipole will experience a weaker field than the other, resulting in a net force. The direction of the force does not depend on the direction (the polarity) of the electric field.

As the radius of the droplets $R_d \approx 2.5$mm is much less than the characteristic length of the idealized plane of charge $L, H \approx 25$mm, we assume that that the effective dipole moment method is valid for our case, and the multipolar effects can be ignored.

The translation force, $\mathbf{F}$ on a dipole μ (whether induced or permanant) in a nununiform field is given by

$$F = \mu \cdot \nabla \mathbf{E}$$

where $\mathbf{E}$ is the field acting on the particle. The dipole moment of a spherical particle in a dielectric medium is

$$\mu = \nu \mathbf{P} = \frac{4}{3}\pi a^3 \mathbf{P}$$

where ν is the volume, a is the radius of the paticle, $\mathbf{P} = (\epsilon_{air} - 1)\,\epsilon_0 \mathbf{E}$ is the polarization per unit volume, where ϵ_{air} is the relative dielectric constant of the medium. The excess polarization of the sphere is

$$\mathbf{P}_e = (\epsilon_{sphere} - \epsilon_{air})\,\epsilon_0 \mathbf{E}_{iz} = \frac{3\epsilon_{air}}{\epsilon_{sphere} - 2\epsilon_{air}}$$

Accordingly μ, the effective dipole moment of the sphere is

$$\mu = 4\pi a^3 \left(\frac{\epsilon_{sphere} - \epsilon_{air}}{\epsilon_{sphere} + 2\epsilon_{air}} \right) \epsilon_{air} \epsilon_0 \mathbf{E}$$

and the translation force, $\mathbf{F}$ is

$$\begin{aligned} \mathbf{F} &= \mu \cdot \nabla \mathbf{E} && (1.1) \\ &= 4\pi a^3 \epsilon_{air} \epsilon_0 \left(\frac{\epsilon_{sphere} - \epsilon_{air}}{\epsilon_{sphere} + 2\epsilon_{air}} \right) \mathbf{E} \cdot \nabla \mathbf{E} && (1.2) \\ &= 2\pi a^3 \epsilon_{air} \epsilon_0 \left(\frac{\epsilon_{sphere} - \epsilon_{air}}{\epsilon_{sphere} + 2\epsilon_{air}} \right) \nabla E^2 && (1.3) \end{aligned}$$

So the dielectrophoretic force is proportional to the volume, to the difference between the dielectric constant and that of the sorrounding medium, and to the gradient of the square

where $\mathbf{E}_{iz}$ is the internal electric field of the sphere in the direction of the external field. [notes about interenal electric field of a sphere].

$$f_{EP} = qE$$

and

$$f_{DEP} = 2\pi R_{drop}^3 \epsilon_{air} K \epsilon_0 \nabla |E|^2$$

1.2. *Droplet trajectories*

Scales for terminal velocity with Coulomb force, and DEP force. Going to a rigid body model from N-S.

FIGURE 6. Model outputs

By applying Newton's Second Law of Motion to a single spherical particle moving relative to the surrounding fluid, the differential equation describing the droplet trajectory can be derived

$$m\frac{d^2y}{dt^2} = \mathbf{F}_{EP} + \mathbf{F}_{DEP} + \mathbf{D}$$

2. Experimental methods

Description of drop tower operations.

2.1. *Superhydrophobic surfaces*

Wetting hysteresis. Methods of fabrication, comparison of wetting properties. Comparison of jump velocities between surfaces. Methods for determination of properties, roll-off angle, contact angle using *SE-FIT*. Cassie-wenzel transition. Damping. Droplets are dyed red to improve the quality of image thresholding when digitizing the droplet trajectories during data reduction.

2.2. *Data reduction*

Digitization of droplet trajectories requires several steps of post-processing. Video is first decomposed into a sequence of still images. Trajectories are captured using the particle tracking module in *Fiji*[ref], a derivative of the popular *ImageJ*[ref] package for scientific image analysis. The series of still images is cropped, and the background (that is, the low-entropy pixels) of the series are removed using a builtin "rolling ball" algorithm. Each still is then split into its constituent RGB maps. In this case the green channel images contained the most information, so these were then globally thresholded using the Triangle algorithm to recover a map of the pixels corresponding to the droplet's approximate position in the original still. Finally ellipses are fitted to the pixel map stepping through the time series to determine the positions of the centroid, and the semi-major and minor axes of the droplets during the drop. The results of the particle capture in *Fiji* are shown in Figure 8.

FIGURE 7. SEM images for sandpaper and laser etched acrylic surfaces

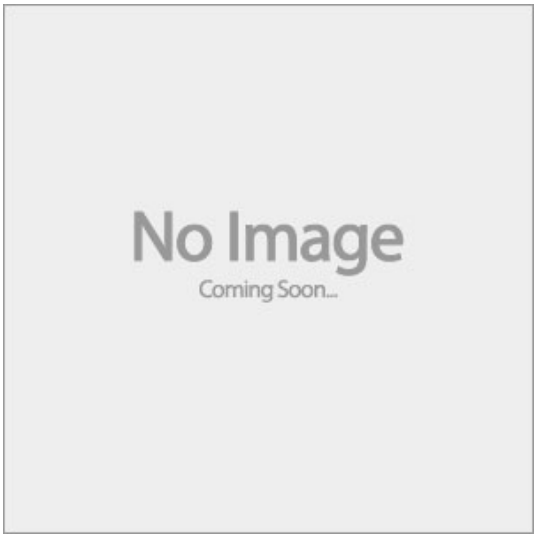

FIGURE 8. Particle tracking before and after

2.3. *Surface charge density*

Surface potentials of the superhydrophobic surfaces were measured using a *Simco-Ion* FMX-004 electrostatic fieldmeter, in low-range mode measured from 25 ± 1 mm above the axis of symmetry. In this mode the electrostatic fieldmeter can measure surface potentials of ± 3.00 kV with ± 10 % accuracy.

The superhydrophobic surfaces become charged when a new layer of PTFE is deposited on the surface, they are dried under a fume hood for a period of 30 minutes to an hour, and then are washed with distilled water. In this way surface potentials $\mu = 0.4$kV, $\sigma = 0.2$kV are attained, corresponding to surface charge densities of [numbers]. The exact charging mechanism acting in this case is unknown but the authors suppose the source of the charge is net charge separation by the breakup of an electrical double layer

as water is washed off of the surface during their preparation, with trapped charges left on the pillars in the Cassie-Baxter area of the surface[ref]. Spontaneous contact charging of PTFE by water is a well known phenomenon[ref][ref][ref]. It is supposed that the functional mechanism forming the double layer is electrosomosis of negatively charged ions across the droplet interface to the PTFE surface[ref], though there is apparently controversy[ref].

Variance within a single hydrophobic surface is sometimes very large (large shooters might have a typical strength distribution mode in the dozens of volts, but with 1-3 kV 'hotspots'). This tendency is exaggerated for non-symmetric shooter geometries.

Observed field strength (measured at 25 mm or 1" from any given surface) was typically in the range of 10-150 V (with a negative polarity). Some outliers were found in the 1-3 kV range. PTFE treatments, and forced air without PTFE drying have the effect of increasing static charge on average. ABS, 3D printed resin and sandpaper surfaces have weaker fields on average than the acrylic, but often still in the low hundreds of volts range.

Field strength was observed to decay exponentially with time; one observation noted a laser etched acrylic hydrophobic surface with an initial uniform 3 kV field decay to 2 kV after about 1 hours time, and decay further to roughly 1 kV about 18 hours later. Air is slightly conductive when ions are present. This implications for the gradual process of charge redistribution across insulating surfaces. Good insulators leak and redistribute charge slowly without the presence of air ions. Theoretically this is true even in the presence of high humidity, as the conductance of most plastics is unaffected by humidity without condensation, due ultimately to the conservation of charge. With the presence of a water film any insulator will immediately discharge. The exponential behavior is also well evidenced for ionized air blower acquired for this research. Initially high voltages can be reduced to the hundreds of volts range in seconds, but further weakening the field to the tens of volts takes minutes.

2.4. *Droplet net charge*

Since, by the earlier scaling, we presuppose the source of the droplet bouncing behavior to be primarily Coulombic in origin (as opposed to dielectrophoretic), the droplet must have some net charge in addition to the charge induced by the electric field. To measure this charge concurrent methodologies were used. The first method of determining the droplet net charge is observation of the deflection of the droplets in the region of a known uniform field in a fashion inspired by Milikan's famous experiment to determine the fundamental charge of the electron [ref]. A uniform, non-rotating field $\mathbf{E}$ =kV/m was set up between two parallel, insulated, 120X120mm polished aluminum plates, positioned [number] mm apart using a $\approx$ 700Vdc source. Something about the AC component. Droplets were jumped in freefall from a sandpaper superhydrophobic surface placed between the plates. The surface was first deionized using a balanced *Ptec* IN5120 DC air-ionizer to remove the effect of surface charge of the superhydrophobic surface from perturbing the otherwise uniform field set up between the parallel plates. A schematic of the parallel plate drop apparatus is shown in Figure 9. Since the droplet initial velocity U_0 is parallel to the electric field, the droplets are inertial in the direction of the electric force, and we can determine the magnitude of the droplet charge by a balance of Coulombic force and inertia given by the equation of motion

$$\frac{d^2y}{dt^2} = q\mathbf{E}.$$

[plus image charges, green's function]

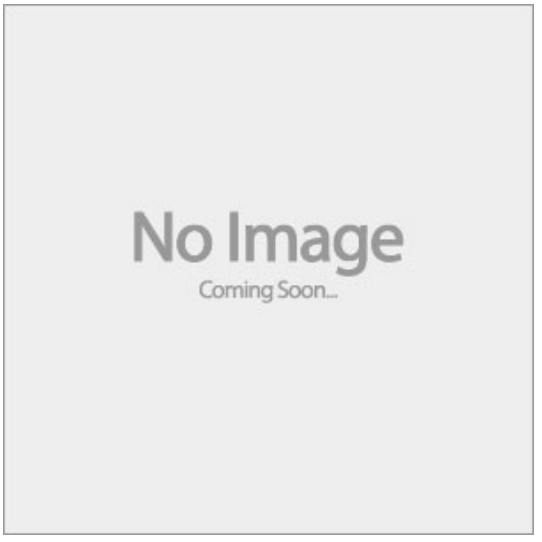

FIGURE 9. Parallel plate experimental apparatus.

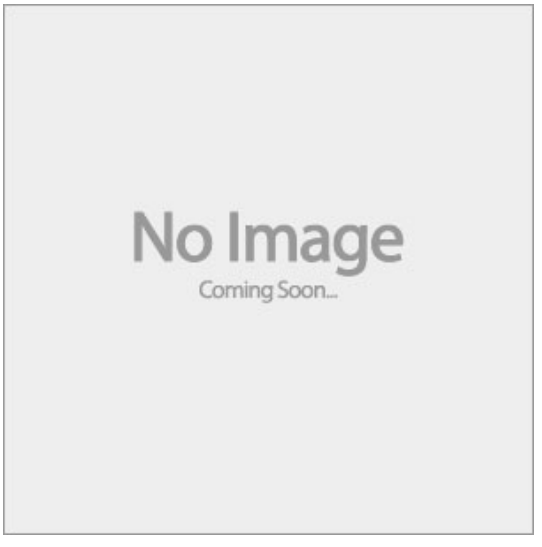

FIGURE 10. Parallel plates: Droplet net charge vs volume.

Since the drag is negligible in the inertial limit we can find the charge q by fitting a second-order least squares polynomial to the measured droplet positions, equating the y^2 term to the constant acceleration, and dividing by the known, constant magnitude of the electric field. From a survey of literature we suppose the droplet charge, if they are indeed charged by contact with PTFE, to be some function of the droplet volume and the residence time on the superhydrophobic surface. But since the characteristic charging time for the droplets is also a function of droplet volume, and [is shown to have a time constant dramatically bigger smaller than that of a typical experimental timescale] we look only for the charge as a function of volume. However, sweeping though droplet volumes over a series of drop tower experiments we find little correlation between droplet volume and net droplet charge. This is shown in figure 10.

All current hydrophobic surfaces in use in the DDT use PTFE spray treatments.

However, sessile droplets can acquire net positive electrical charge by contact with PTFE surfaces through electro-osmosis of ion species. Even in the case of the hydrophobic surface being meticulously grounded with the use of a benchtop ionizer, droplets with non-zero net charge will repel each other dung the jump. Thus, to complete a survey of the typical electrostatic perturbations on droplet kinematics as experienced in the DDT an estimate of charge accumulation on droplets is needed.

The general approach to estimating the droplet charge is by jumping the droplet in the presence of a uniform electric field and measuring the acceleration towards the negative electrode of a parallel plate capacitor per Equation **??**. This approach is similar to Robert Millikan's original experiment to determine the fundamental charge of an electron. Control of the plate spacing with a known voltage bias allows for an accurate calculation of the magnitude and direction of the electric field.

A 200-880 V AC source (an inexpensive electric flyswatter purchased at Harbor Freight) with a full wave bridge rectifier circuit was prototyped on perf-board for initial experiments to measure droplet charge. The circuit was analyzed on an laboratory oscilloscope to verify that the AC component of the signal was appropriately small (13 mV at 35 kHz). Current was determined to be a relatively safe 80 μA. The high-voltage source terminals were led to two parallel polished 150x150 mm aluminum plate electrodes. The electrodes were mounted on an extruded aluminum rail for ease of adjustment. All droplet charge experiments were conducted with an electrode spacing of 28.30 mm. With this spacing the calibrated electric field between the plates was 3.5e4 V/m. The electrodes were electrically isolated from the drop rig by two alternating layers of 4 mm thick laser cut acrylic sheet and Kapton tape. Potential across the plates was measured periodically with a load-impedance corrected multimeter to account for battery depletion. The typical capacitor rise time of the plates was measured to be 1.4 s, thus to make the most economical use of the brief window a micro-gravity a weighted switch was set by hand prior to the drop to close the high-voltage circuit, but which passively safed the system at the resumption of 1-g conditions in the tower. The drop apparatus is shown in Fig.

A brief screening experiment was conducted which alternated the polarity of the field by switching the positive and negative terminal leads between plates. Qualitative observations of droplet electrode preference seem to indicate that the assumption of small polarization stress was well founded. Following this a orthogonal array 3^2 factorial design experiment with two replicates was conducted to test the effect of varying droplet volume and surface stay time on net charge at the time of jumping. It was hypothesized in accordance with previous studies **?**, that net charge would increase for levels of both factors. The results of the factorial experiment are presented in Fig. **??**. ANOVA analysis of the linear multiple regression model for the data set indicates that neither droplet volume ($p = 0.105$), nor surface stay time ($p = 0.358$) is significant at the 95% confidence level. The overall model F-statistics (2.177 in 2 and 13 degrees of freedom), and coefficients of determination ($r^2 = 0.2509$) indicate that the linear model neither fits the data particularly well, nor does it offer an improvement over the mean model. The mean charge was determined to be positive 2.3e-11 C, with a standard deviation of 1.8e-11 C.

The failure of the model to describe the data raises interesting questions about the validity of our initial assumptions. Typical Reynolds numbers ($R_e = 280$ average) indicate the general validity of the assumed quadratic drag model. The drag scale quantity given by Eqn. **??** was much less than 1 for all test runs, with mean value of 1.0e-2 and a standard deviation of 2.0e-3, which adds credence to a force balance of pure inertia and electrostatic force.

An additional source of concern was that droplets in three of eighteen runs exhibited accelerations opposite to the expected direction. There is no pattern to the distribution of anomalous droplet accelerations, as they all occurred at unique level combinations. There are only four obvious ways of explaining this anomaly, and perhaps the problems of the general model as well. The first is that the electric field is in fact non-uniform and polarization stress is non-negligible. This option seems unlikely owing to the fundamental design of the experimental apparatus. If we ignore dielectric properties of the air between the plates, the electric field lines should be parallel and have equal magnitudes throughout the experimental area. A second possibility is that the few contrarian droplets actually accumulated net negative charge, instead of the net positive charge to be expected on the basis of evidence from some of the aforementioned studies. While this is not impossible in principle, it raises the spectre of new unknown confounding variables at work with the hydrophobic surfaces themselves. A third possibility is that another force neglected in the analysis, with some component in the direction opposite of the electric field, has an order one magnitude.

A final possibility lies with the means used to measure the acceleration of the droplets (and thence the electrostatic force). The droplet time variant position, measured using manual tracking methods in NASA Spotlight image analysis software, was used to calculate discretized instantaneous velocities for the length of the trajectory. The slope of the linear regression of instantaneous velocity versus time was taken to be the average acceleration of the droplet. Admittedly this approach does not lend itself well to accuracy as small errors during the manual tracking process are integrated twice in the final result. The average coefficient of determination for the population of instantaneous velocity regressions is 0.27 (with a range of 3.0e-4 to 0.75), and the anomalous data is generally more scattered than this mean value. If this is the source of the anomalous accelerations, and the error is random and normally distributed then the accelerations should, in principle, disappear with further repeated measures.

Use of concurrent methods for measuring the charge could resolve the question of the anomalous accelerations. This can be done by direct measurement of droplet using a field meter and Faraday cup. Unfortunately, such an approach requires specialized, highly-sensitive field meters. At present the expense of such sensors renders this approach impractical. Another possible approach is to compare experimental droplet interface curvature in the presence of a controlled electric field in 1-g to those computed using SE-Fit software find an equivalent elkectrostatic Bond number and thus the electrostatic body force acting on the droplet.

The droplet positive net charge developed by contact with a PTFE surface corresponds to findings elsewhere in literature **? ? ?**. The smallest droplet size treated in the present work is several times larger than the largest in any of comparable study. The most relevant comparison found droplet static charge of 2.5e-10 C for 10 μL droplets charged by pipetting from a PTFE tipped needle **?**. The present results mean charge level of 2.3e-11 C is, within error, roughly six times smaller than the cited study.

A second approach to determining the net droplet charge is by direct measurement in a shielded Faraday cup using an extremely high input resistance electrometer, specifically a *Keithly* 616 digital electrometer. [note on operational philosophy, data collection]. Correlation of net charge to droplet volume is shown again for in figure 11.

Discussion on discrepancy between the two approaches. (Magarvey & Blackford ????)

3. Results

- Acceleration histories

FIGURE 11. Electrometer: charge vs. volume.

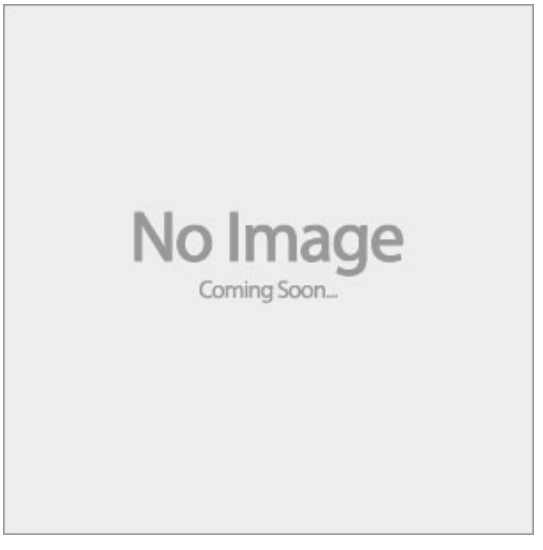

FIGURE 12. Acceleration histories compared for different $q/m\sigma$

- ANOVA to compare variance of jump velocity to variance in charge or nonuniformity of field between tests... Electrowetting.
- Comparison of the model to experimental data
- Gravitational analog, validity of the stability model, bifurcation, linear stability

4. Further Work

Concepts for other geometries. N-body interactions.

REFERENCES

FIGURE 13. Comparisons to the model

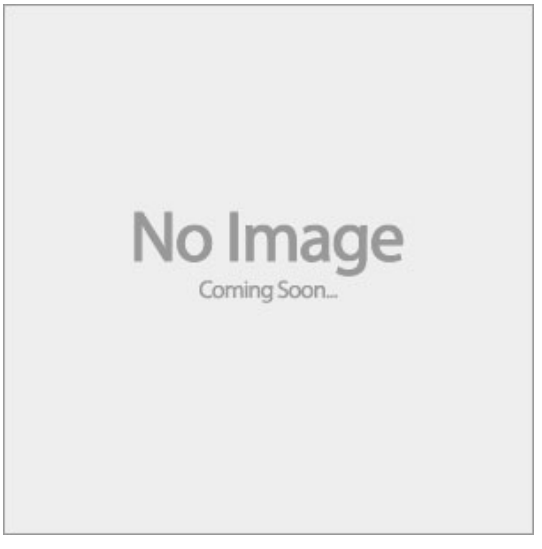

FIGURE 14. Gravitational analog

MAGARVEY, R. H. & BLACKFORD, B. L. ???? Experimental determination of the charge induced on water drops **67** (4), 1421–1426.

Appendix A.
Surface charge density

Since the laser-etched acrylic, and sandpaper superhydrophobic surfaces are both dielectric materials there are some additional considerations for determining the surface charge density. Firstly, for an insulated conductor A with charge q, the charge distribution in equilibrium will be such that the field on the interior of the conductor is zero, with field lines being normal to the surface and the integral of the field strength $\mathbf{E}$ from any

FIGURE 15. Conductive S.H. surface apparatus schematic.

FIGURE 16. FEM solution in *Agros2D*.

point P in or on the conductor to a ground point G is a constant given by

$$V = \int_P^G \mathbf{E} \cdot da,$$

where V is the voltage or potential of the conductor (or alternatively, the surface voltage potential). The voltage V and the charge q are proportional and q is usually given by

$$q = CV,$$

where C is the capacitance of the insulated conductor and is determined by the conductor's size and shape, and its placement relative to the conductors and ground. However, the case of a charged insulator departs significantly from that of the insulated conductor. Here we have the possibility of the density and net polarity of the charge varying as a

function of position about the surface. The field of the interior may not be zero, and the field lines are not necessarily normal to the the surface. The integral of the field strength from a point on or in the insulator to ground is usually different from point to point. In general the surface voltages will vary from point to point on an insulator (including point on the interior of the insulator. Therefore it is not possible to uniquely define the voltage of a charged insulator, except in certain contrived cases (notably the the potential of a uniformly charged sphere positioned infinitely far away from any conductors). It follows that there is no definition for the capacitance of an insulator as well. Though insulative sheets may store charge and discharge in the manner of capacitors, this discharge is never particularly complete.

There are two cases where we can make meaningful quantitative measurements of state variables for charged insulators: we can measure the electric field arising from the charge, and possible the total charge for uniformly charged free insulative sheets, and uniformly charged insulative sheets backed by a grounded conductor. To do this we can use field meters and non-contacting voltmeters. If the field strength indicated on the meter is $\mathbf{E}$, the charge density σ on the part of the insulator in the front should be $\sigma = \epsilon_0 \mathbf{E}$. If a non-contacting voltmeter is placed a at a distance d from the sheet, then the surface voltage V_s indicated on the meter is given by

$$V_s = d\mathbf{E} = d\frac{\sigma}{\epsilon_0}.$$

An ideal approach to determining surface charge on a dielectric surface is to screen perturbing effects of external electric fields. This is partly accomplished by grounding the fieldmeter, and by placing the dielectric sample on a grounded conductive plate backing. In this case the surface charge density is determined from

$$\sigma = \frac{V_s \epsilon}{l},$$

where l and ϵ are the absolute permittivity and thickness of the dielectric surface respectively. The measured surface voltage is a function of position away from the charged dielectric. In most cases this function is relatively constant at a distance about 1-2 cm away from the surface (there is some measurement error in surface voltage due to small mispositioning of the electrostatic fieldmeter, say by ± 1 mm) and add it to the precision error of measurement in V_s. The measured surface voltage can also be compared to the analytically derived surface voltage determined from the analytical expression for the electric field from above, and to those determined from finite element solutions to poisson's equation on the domain in question. [Notes about *Agros2D*] The surface voltage is shown schematically as a function of the measurement distance in Figure 17 for a sample charge density $\sigma =$.

A further consideration is the possibility of the change in total charge during a typical experimental timescale. If we consider the drop rig to be a ground (which seems reasonable given that the rig is isolated from true ground, but is at some reference voltage with respect to the surface charges on the dielectric, it also has an abundance of free charge carriers, that it, it is conductive), then there will be both bulk and surface decay of the charge on the dielectric. The evolution of the charge can be approximated by

$$\sigma = \sigma_0 e^{\frac{-t}{\epsilon \rho}},$$

where σ_0 is the initial surface charge density, and ρ is the bulk resistivity (which can also be reframed in terms of conductivity by $\rho = 1/\gamma$, where γ is the conductivity). For an example case of a surface with an initial surface charge density $\sigma = 2.4 \cdot (10^{-6})$

FIGURE 17. Measured surface voltage versus position.

C/m^2, relative permittivity $\epsilon = 3.5$ and bulk resistivity $\rho = 1.6 \cdot (10^{16})\ \Omega/cm$ such as with the case of 1/4" continuous cast acrylic sheet, then the time constant $\tau = \epsilon\rho$ is approximately 5000 s, which is a great deal longer than the typical time period for of a drop tower experiment.

Appendix B.
Data smoothing

In trying to recover the kinematic variables from the droplet trajectories we encounter a difficulty in the noise of the position data:

- Notes from Wood, "Data smoothing and Differentiation procedures in Biomechanics"
- Signal-to-noise ratio is $\mathcal{O}(f)$ for $\frac{df}{dt}$ and $\mathcal{O}(f^2)$ for $\frac{d^2f}{ft^2}$. Refs 5, 14, 49, 95.
- Error sources include misalignment of the camera, perspective due to objects (subject or reference scale) being out of the photographic plane, precision limits in digitization. Some of these errors are systematic in origin and introduce consistent biases into the data (e.g. coherent spectral sources, rather than truly stochastic noise). These systematic sources of error include inaccurate scales among others. Data smoothing tends not to help with the systematic errors in that they are usually of lower frequency than the signal (and here we are trying specifically to filter high frequency noise).
- Random errors are assumed to have a Gaussian distribution (by the central limit theorem), and are independent of the signal (which inherently results from a deterministic process).
- Central differences are usually a better approximation of the instantaneous value of the true derivative of the signal, as compared to forward differences. The finite differences are mathematically equivalent to passing a quadratic interpolating polynomial through the three points of the central difference (assuming the window size of the central difference is $N = 3$, larger windows are possible). To obtain an approximation for the m^{th} derivative of $f(x)$ at least an m^{th} order polynomial is required.
- One straightforward approach to getting the position derivatives is to fit a least

FIGURE 18. Filtered or fitted droplet trajectories compared to raw data.

squares polynomial to the global position data, and analytically differentiate. This is a simple to apply, and therefore quite popular approach. The order of the polynomial is picked from theory, by ANOVA, or comparison of the residuals to determine goodness of fit for $m + 1$. It should be stress that there are significant drawbacks with this approach: firstly is that when derived values depend on both accuracy of segmented displacement-time data and body segmental parameters (segmental masses and center of mass locations), then the errors are confounded and it is difficult to evaluate the accuracy of the derivative. Secondly, statistics used to asses agreement between curves are either in-appropriate because they aim to represent fundamentally deterministic processes in probabilistic ways (as would be the case using a product-moment correlation), or there is no test of significance (as is the case with a mean-errors correlation). Finally High order effects are easily lost by a global polynomial fit for time series containing multiple length scales or frequencies, as is the case here [ref].

In lieu of global polynomial fits we can attempt at finite differencing the data after the application of smoothing filters. Some of these approaches are global and/or recursive whereas other approaches are applied locally. Each approach has various natural advantages and disadvantages. A number of approaches were implimented in *Python* or imported from the scientific computing package *SciPy*[ref] and compared for a test set of trajectory data; these methods include convolution with the derivative of a Gaussian kernel, Wiener filtering, smoothing splines, Butterworth low-pass filtering, total-variance regularization, and Savitsky-Golay filtering. Qualitatively comparing these smoothing methods we find that we loose too many data points in the smoothing process, the variance remains large (especially in higher derivatives), large amplitudes are overly smoothed by repeated filtering passes, or there are significant end effects for most of these methods. A comparison of these smoothing approaches on a representative trajectory data set are shown in Figure 18. The power spectra for the same data are compared for these methods in Figure 19.

Savitsky-Golay filtering seems to produce the smoothest derivatives without overfitting of otherwise misrepresenting the underlying signal. The Savitsky-Golay algorithm

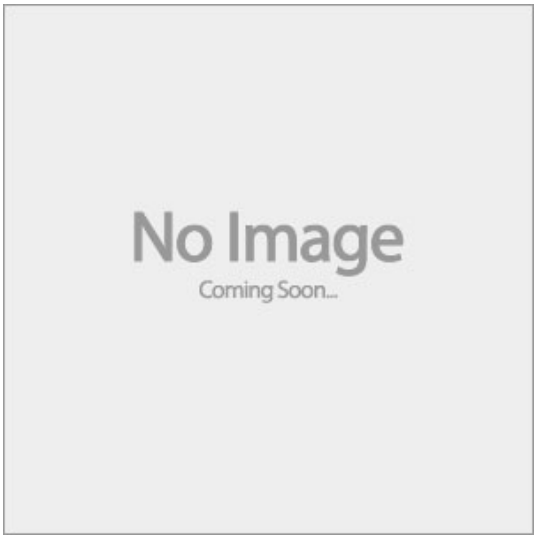

FIGURE 19. Power spectra of the filter methods compared.